CANCER GENOMICS & PROTEOMICS 2: 25-36 (2005)

# A Display Thiol-Proteomics Approach to Characterize Global Redox Modification of Proteins by Selenium: Implications for the Anticancer Action of Selenium

EUN-MI PARK[1,3], KYOUNG-SOO CHOI[1], SOO-YEON PARK[1], EUNG-SIK KONG[1], KE ZU[2], YUE WU[2], HAITAO ZHANG[2], CLEMENT IP[2] and YOUNG-MEE PARK[1]

*[1]Department of Cellular Stress Biology and [2]Department of Cancer Chemoprevention, Roswell Park Cancer Institute, Elm & Carlton Streets, Buffalo, NY 14263, U.S.A.; [3]Department of Chemistry, University of Incheon, Incheon, 402-749, Korea*

**Abstract.** *Background: The generation of a monomethylated selenium metabolite is critical for the anticancer activity of selenium. Because of its strong nucleophilicity, the metabolite can react directly with protein thiols to cause redox modification. These chemical changes have never been examined systematically before because of the lack of a reliable methodology to study reactive protein thiols globally in cells and to quantify their redox status. Materials and Methods: PC-3 human prostate cancer cells were treated with methylseleninic acid (MSA) for 0.5, 1, 2, 3, 6, 12 or 24 h. A reactive thiol specific reagent, BIAM, was used to detect the extent of global redox changes on a 2D gel electrophoresis display. The data were analyzed by the Self Organizing Maps clustering algorithm. Protein identification was done by MALDI-TOF and ESI-tandem mass spectrometry. Results: Out of a total of 194 reactive thiol-containing protein spots on the 2D gel display, 100 of them (cluster 1) were not sensitive to MSA modulation. The remaining 94 were categorized into three distinct patterns. Cluster 2 (60 proteins) showed an immediate and sustained loss of reactive thiols for at least 24 h; cluster 3 (19 proteins) showed a transient loss of reactive thiols followed by a rapid rebound; and cluster 4 (15 proteins) showed a transient gain followed by a rapid return to normal. In contrast, there were minimal protein redox changes in control cells (not treated with MSA) over the same period of time. A total of 85 proteins were identified of which 40 were in clusters 2 to 4. The proteins which are sensitive to redox modification by MSA are distributed in various subcellular compartments. Western blot analysis showed that a number of chaperones were significantly induced by MSA. Conclusion: Global redox modification of proteins can be a major driving force of cellular stress, since these changes are likely to lead to protein unfolding, misfolding or aggregation. The induction of chaperones in cells treated with MSA is consistent with this interpretation since chaperones are charged with rescuing misfolded proteins. The above scenario is discussed in relation to an adaptive response which ultimately determines how cells respond to treatment with selenium.*

The anticancer activity of selenium is well documented (1). Both inorganic and organic selenium compounds, as exemplified by selenite and selenomethionine, respectively, are effective in suppressing tumorigenesis in animal models. As proposed originally by Ip and coworkers (2-4), the metabolism of selenite or selenomethionine to methylselenol ($CH_3SeH$) is important for their anticancer activities. Methylselenol is highly reactive, difficult to prepare, and cannot be tested as is *in vitro*. In order to obviate this problem, a stable metabolite called methylseleninic acid ($CH_3SeO_2H$, abbreviated to MSA) was developed specifically for cell culture studies. Once taken up by cells, MSA is reduced rapidly to $CH_3SeH$ through non-enzymatic reactions (5). *In vitro* studies with human prostate cancer cells showed that exposure to MSA results in cell cycle arrest and induction of apoptosis (6-11).

At physiological pH, methylselenol is present as anionic methylselenolate. Most protein cysteine residues would not react with methylselenolate because they generally exhibit a $pK_a$ value of 8.0-8.5. But some protein cysteine residues exist as thiolate anion at neutral pH, because their $pK_a$ value is lowered as a result of the influence of neighboring nucleophilic groups, and the thiolate is often stabilized by salt

*Abbreviations:* MSA, methylseleninic acid; BIAM, N-(biotinyl)-N'-(iodoacetyl) ethylenediamine; SOM, self-organizing maps; ER, endoplasmic reticulum.

*Correspondence to:* Young-Mee Park, Department of Cellular Stress Biology, Roswell Park Cancer Institute. e-mail: youngmel.park@roswellpark.org or Clement Ip, Department of Cancer Chemoprevention, Roswell Park Cancer Institute, Elm & Carlton Streets, Buffalo, NY 14263, U.S.A. e-mail: clement.ip@roswellpark.org

*Key Words:* Thiol-proteomics, redox modification, selenium anticancer action.

bridges to positively-charged moieties (12,13). By virtue of the negative charge, thiolates have enhanced reactivity and are called "reactive thiols". Many vicinal thiols are reactive thiols. Under oxidative stress condition, a reactive thiol could easily lose an electron to become a thiyl radical (14,15), which can then react with methylselenolate to form an activated selenenylsulfide intermediate. The latter is susceptible to attack by a second thiol to form an intramolecular disulfide (16). Due to its strong nucleophilic nature, methylselenolate also readily reacts with protein disulfides and converts them to sulfhydryl groups (16). From the above description, it is apparent that the interaction of proteins with methylselenolate could result in either a gain or a loss of reactive thiols, depending on the reduction potential of the redox couple. These modifications have never been examined systematically before because of the lack of a reliable methodology to quantify protein reactive thiols globally in cells. In the present study, we aimed to: (i) examine the thiol proteome profile in human prostate cancer cells using a biotinylated iodoacetamide-based display approach, (ii) investigate the kinetics of protein thiol modification by MSA using a pattern recognition algorithm, and (iii) identify these selenium-sensitive thiol-containing proteins by MALDI-TOF and ESI-tandem mass spectrometry. An equally important aspect of the paper is to discuss how protein redox modification might serve as an underlying mechanism in mediating the anticancer action of selenium.

## Materials and Methods

*Cell culture and treatment condition.* PC-3 human prostate cancer cells were obtained from the American Type Culture Collection (Manassas, VA, USA). They were cultured in RPMI 1640 medium supplemented with 10% fetal bovine serum, 2 mM glutamine, 100 units/ml of penicillin and 100 μg/ml of streptomycin (6). MSA was synthesized as described previously (5) and added to the culture medium at a final concentration of 10 μM. Cells were processed for protein reactive thiol labeling after 0.5, 1, 2, 3, 6, 12 or 24 h of exposure to MSA. In a parallel experiment, control cultures without MSA treatment were processed similarly after 3, 6 or 24 h.

*Reactive thiol labeling with N-(biotinyl)-N'-(iodoacetyl) ethylenediamine (BIAM).* Proteins with reactive thiols were labeled with a thiol-specific reagent, BIAM, according to the method of Kim *et al.* (17) with minor modifications. Briefly, cells were exposed directly to 100 μl of lysis buffer containing 20 μM BIAM (Molecular Probes, Eugene, OR, USA) in a hypoxic chamber. The lysis buffer consisted of 50 mM 2-(N-morpholino) ethanesulfonic acid (pH 6.5), 100 mM NaCl, 0.5% (v/v) Triton X-100, 1 μg/ml leupeptin, and 10 μM phenylmethylsulfonyl fluoride; the buffer was rendered free of oxygen by bubbling with argon gas at a low flow rate for 1 h. Cells were detached from the dish with a cell scraper and homogenized with a glass/glass homogenizer with 10 strokes in an anoxic condition. The labeling reaction was terminated by adding β-mercaptoethanol to a final concentration of 20 mM. The reaction mixture was centrifuged at 10,000 g for 10 min at 4˚C. The supernatant was subjected to 2D gel electrophoresis.

*2D gel electrophoresis and image analysis.* The supernatant was mixed with a rehydration buffer (8 M urea, 2% CHAPS, 1% IPG buffer, and 50 mM DTT) for 2 h at room temperature. It was electrofocused in DryStryps (pH 3-10 NL) with the IPGphore (both from Amersham Biosciences). After electrofocusing, the gel was equilibrated for 15 min with a buffer containing 10 mg/ml DTT, 8 M urea, 2% (w/v) SDS and 30% (v/v) glycerol, and then for another 15 min with a second buffer containing the same ingredients with the exception that DTT was replaced with 25 mg/ml iodoacetamide. Second-dimensional SDS-PAGE was performed on a 12% polyacrylamide gel.

Proteins labeled with BIAM were transferred to a PVDF membrane and detected with HRP-conjugated streptavidin (Amersham) and enhanced chemiluminescence. The image of the thiol-specific-stained blots was analyzed by PDQuest (version 7.1, Bio-Rad) to extract the raw intensity data. The total quantity of internal control spots was used for normalization. A separate portion of the protein extract was subjected to 2D gel electrophoresis, stained with SyproRuby (Bio-Rad), and processed for the subsequent identification of labeled proteins.

*Data analysis by scatter plot and self-organizing maps (SOM) clustering.* The normalized intensity values were transformed to $\log_2$ scale and subjected first to scatter plot analysis. For both the control and MSA data, the scatter plots were constructed by plotting the intensity value of each spot at the zero hour time point (x-axis) against the intensity value of the same spot at a different time point (y-axis). The Pearson's correlation coefficient was calculated using the formula:

$$r = \frac{\sum_{i=1}^{n}(x_i - \bar{x})(y_i - \bar{y})}{\sqrt{\left[\sum_{i=1}^{n}(x_i - \bar{x})^2\right]\left[\sum_{i=1}^{n}(y_i - \bar{y})^2\right]}}$$

Additionally, the normalized intensity values were used to calculate the treatment to control signal ratio for each spot. The $\log_2$-transformed ratios were subjected to unsupervised clustering analysis using the SOM algorithm (18,19). The unsupervised method was used because we had no *a priori* expectation of what kind of clustering pattern would emerge, nor did we make any assumption. This analysis was performed using custom PERL scripts and the GeneCluster 2.0 program from the Center for Genome Research, Whitehead Institute, Massachusetts Institute of Technology, USA.

*Protein identification by mass spectrometry.* Protein spots were analyzed by mass spectrometry after tryptic in-gel digestion. For the initial analysis, we carried out MALDI-TOF mass spectrometry using M@LDI™-LR (Micromass, Beverly, MA, USA). The raw mass spectra were analyzed to obtain a list of monoisotopic peaks using ProteinLynx Global SERVER 2.0 program from Waters (http://www.waters.com). The peptide mass error was limited to 50 ppm. The protein candidates were identified using the National Center for Biotechnology Information (NCBI) database as the search engine. When the search results were ambiguous, the remaining tryptic mixture after MALDI-TOF mass spectrometry was subjected to ESI-tandem mass spectrometry using Q-TOF API US (Micromass).

*Protein annotation and retrieval of information on vicinal thiols.* The sequences and annotations of the identified proteins were retrieved from the Protein database at the NCBI by querying the database

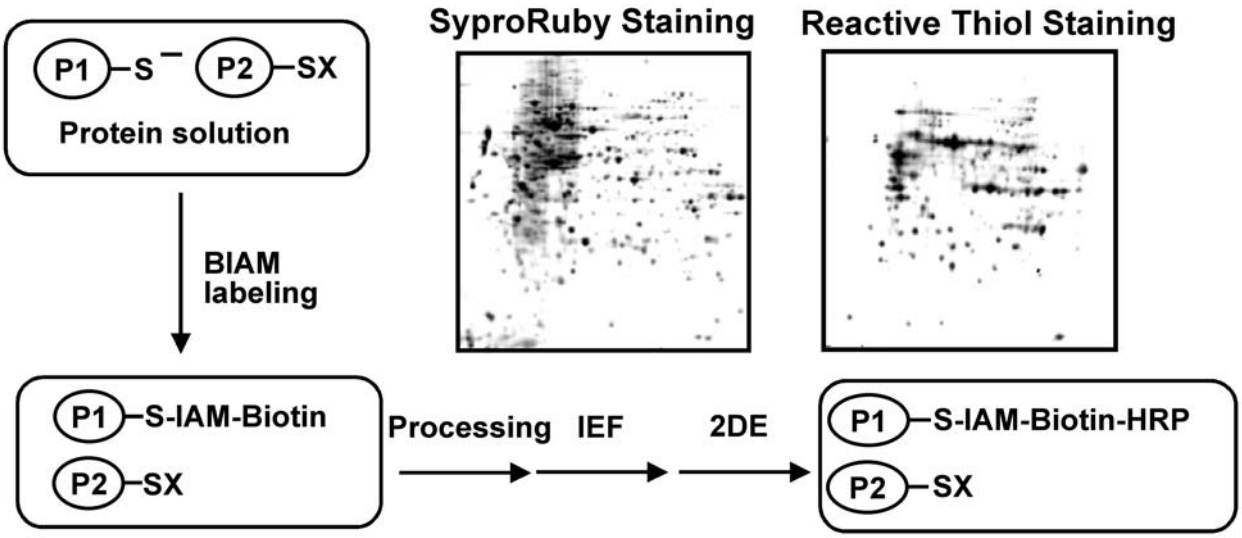


Figure 1. *Schematics and display of BIAM labeling of reactive thiol-containing proteins. Protein extract from PC-3 cells was labeled with BIAM. After 2D gel electrophoresis, one sample was processed for total protein staining by SyproRuby, and another processed for reactive thiol-containing proteins by HRP-conjugated streptavidin.*

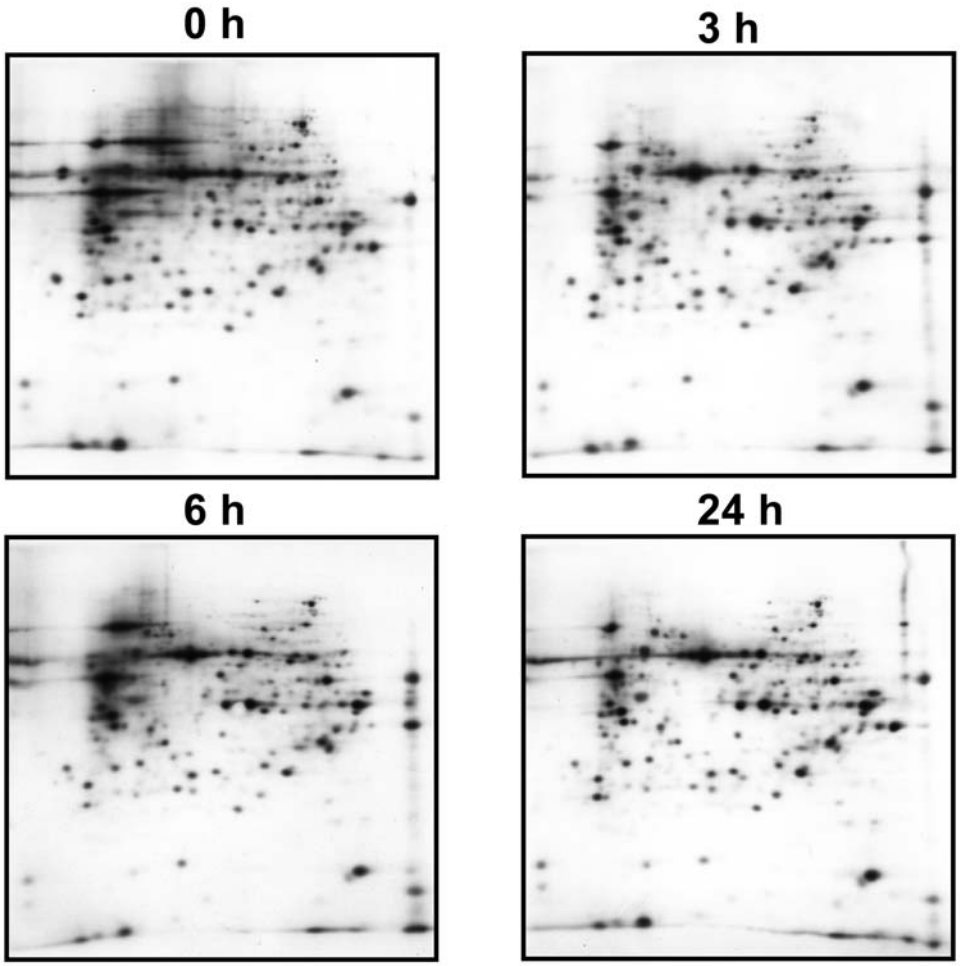


Figure 2. *Thiol-proteome profile of PC-3 cells not treated with MSA. The protein extract obtained at different times of culture was labeled with BIAM, and processed as shown in Figure 1.*

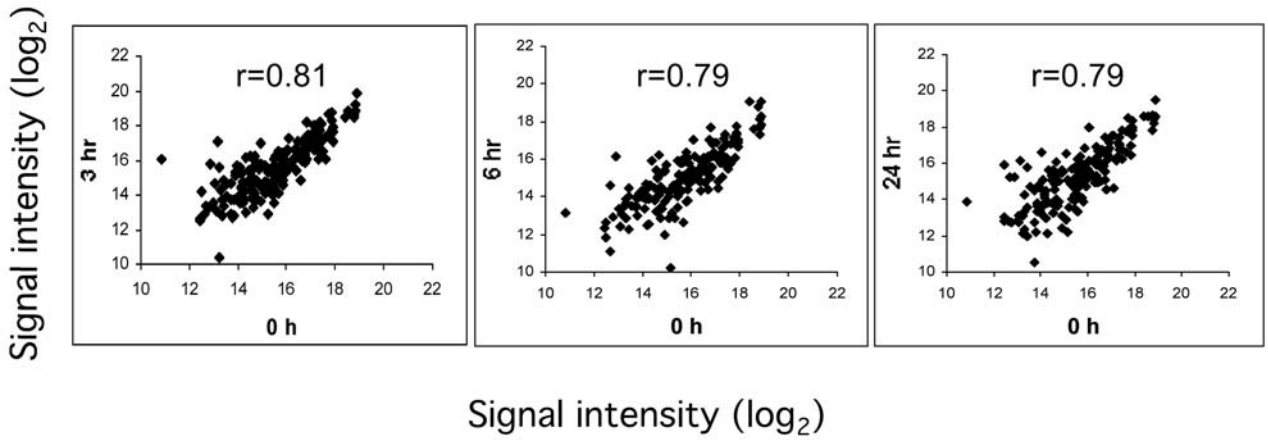


Figure 3. *Scatter plot and correlation analysis of the control data (no MSA treatment).*

with the protein accession numbers. The sequences were analyzed for the presence of vicinal thiols using regular expression. The above analyses were performed with custom PERL scripts.

*Western blot analysis.* Details of the procedure were described previously (6). Immunoreactive bands were quantitated by volume densitometry and normalized against GAPDH as the loading control. The following antibodies (source) were used in Western blots of whole cell lysate: anti-GRP170 (rabbit polyclonal, generously provided by John Subjeck at Roswell Park), anti-GRP78 (rabbit polyclonal from Santa Cruz Biotechnology, Santa Cruz, CA, USA), anti-inducible HSP70 (mouse monoclonal from Stressgen Biotechnologies, San Diego, CA, USA), anti-PDI and anti-HOP-p60 (both mouse monoclonal from Transduction Laboratories, Lexington, KY, USA).

## Results

*Display of BIAM-labeled reactive thiols on 2D gel.* As shown in the schematics of Figure 1, reactive thiols are earmarked by a thiol-specific reagent, BIAM. More specifically, the reagent is biotinylated so that the biotin group now linked to the protein thiol (-S-IAM-biotin) can later react with HRP-conjugated streptavidin to locate the spot on the 2D gel. Since BIAM preferentially reacts with thiolates and not cysteine sulfhydryl groups (Cys-SH), only proteins with reactive thiols are visualized by HRP-conjugated streptavidin and enhanced chemiluminescence. Figure 1 shows a typical SyproRuby staining of total proteins and a typical reactive thiol-specific staining with BIAM. There are noticeably fewer protein spots in the latter compared to the former. The total proteome and the thiol proteome profiles are clearly different. Approximately 35% of total protein spots are consistently labeled by BIAM in our hands.

*Lack of significant changes of reactive thiol proteome profile in control cells not treated with MSA.* BIAM labeling was carried out in control cells at 0, 3, 6 or 24 h. The 2D gel reactive thiol images are shown in Figure 2. In order to facilitate a comparison of the image intensity of each spot at different time points standardized against the zero hour data, we performed a scatter plot analysis to study the variations as a function of time. These plots are shown in Figure 3. Based on the Pearson's correlation coefficient denoted in each panel ($r=0.81$, 0.79 or 0.79 for the 3, 6 or 24 h time point, respectively), it is evident that there were minimal changes in redox modification of proteins during this period. Suffice it to note that since the image intensity is enhanced by chemiluminescence, a coefficient of $\sim 0.8$ is generally regarded as the norm for any control culture based on our experience with similar thiol proteome analysis in various cell types.

*Effect of MSA treatment on protein redox modification.* Cells were treated with 10 μM MSA for 0.5, 1, 2, 3, 6, 12 or 24 h. MSA did not affect growth or apoptosis of PC-3 cells within this time frame (6). The purpose of the experiment was to quantify the subset of proteins sensitive to redox modification by MSA and the manner in which these changes occurred. The results are shown in Figure 4. Within each panel, the triangles and circles denote the spots of which the BIAM labeling intensity was either decreased or increased, respectively, in response to MSA. Not every sensitive spot is marked by a symbol. Otherwise the 2D gel image would have been too cluttered to show what we want to convey. Two key findings emerge from the BIAM labeling data. First, MSA was able to affect the redox status of 94 out of a total of 194 proteins labeled by BIAM. Second, more reactive thiols were lost than gained as a result of MSA treatment (more triangles than circles in each panel). Representative scatter plots of the MSA data at 3, 6 and 24 h are shown in Figure 5. The patterns from MSA-treated cells are clearly different than that from control cells

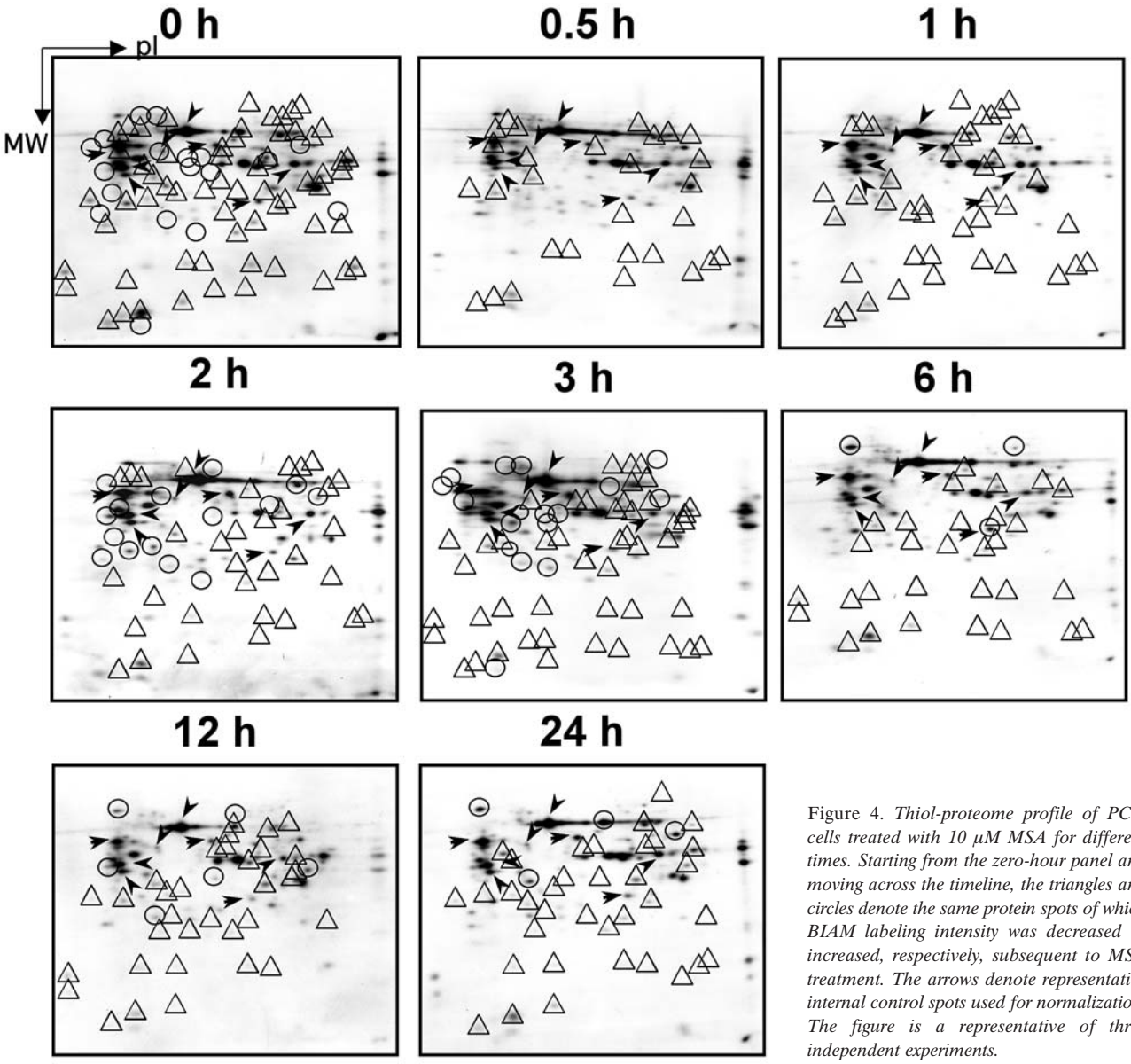


Figure 4. *Thiol-proteome profile of PC-3 cells treated with 10 μM MSA for different times. Starting from the zero-hour panel and moving across the timeline, the triangles and circles denote the same protein spots of which BIAM labeling intensity was decreased or increased, respectively, subsequent to MSA treatment. The arrows denote representative internal control spots used for normalization. The figure is a representative of three independent experiments.*

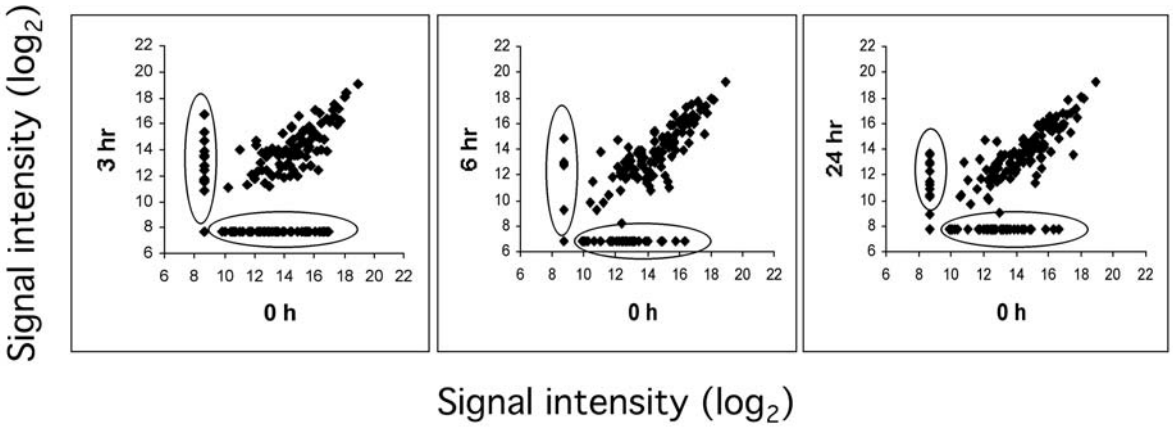


Figure 5. *Scatter plot analysis of the MSA data at selected time points.*

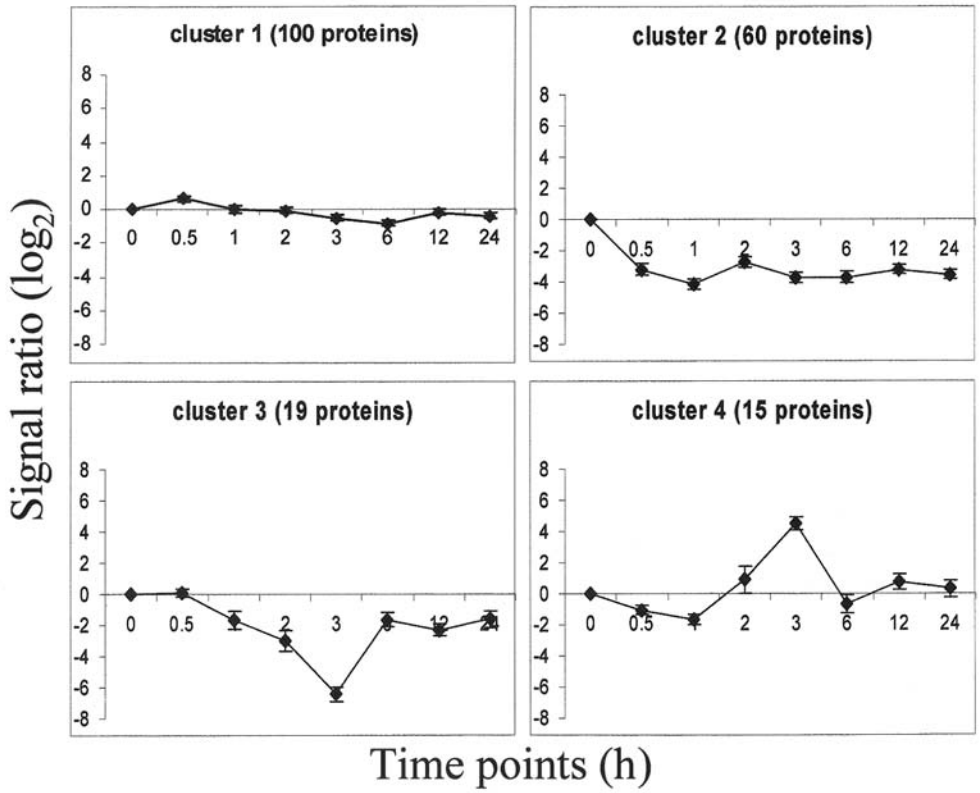


Figure 6. *SOM clustering analysis of the MSA data shown in Figure 4. The Y-axis represents the $log_2$-transformed treatment to control ratio. The error bar represents mean ± SEM of this value.*

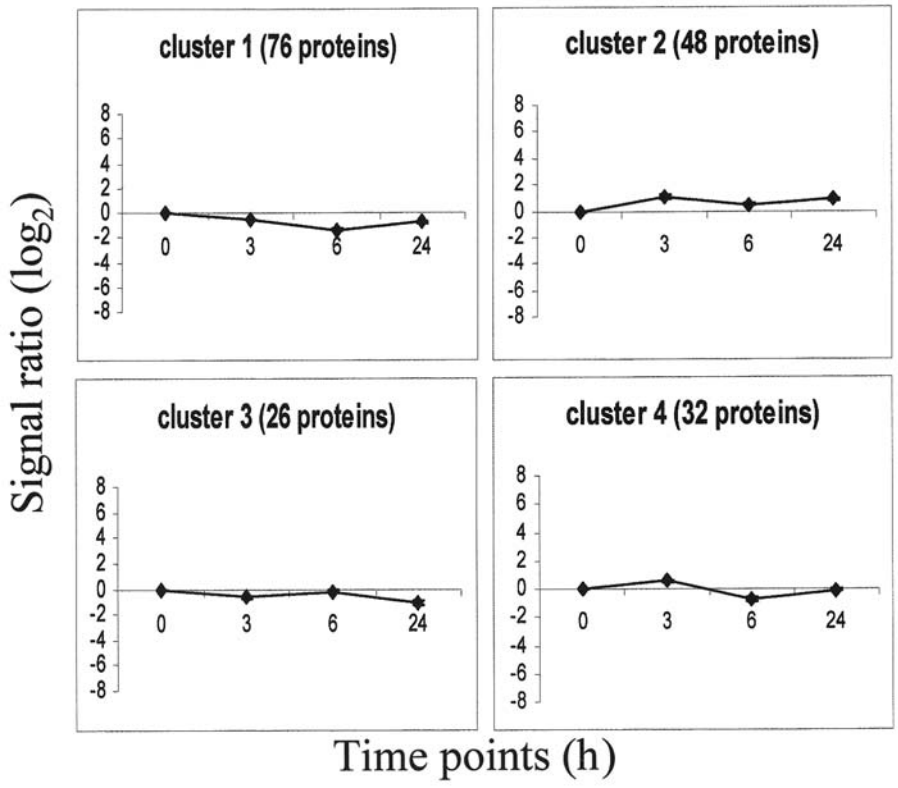


Figure 7. *SOM clustering analysis of the control data shown in Figure 2.*

(compared to Figure 3). There are subsets of proteins with either increased or decreased reactive thiols following exposure to MSA.

In order to obtain further insight into the manner of protein thiol redox changes induced by MSA, we used the Self Organizing Maps (SOM) algorithm to analyze the dataset. The analysis was done based on $\log_2$ transformation of the treatment to control signal ratios at each time point. Four distinct patterns of redox changes emerged from the analysis, as shown in Figure 6. Cluster 1, which consists of 100 proteins or ~51% of the total, exhibited very little change in reactive thiol labeling intensity throughout the course of MSA treatment. Cluster 2, which consists of 60 proteins or ~31% of the total, responded rapidly with an averaged 8-fold decrease of thiol labeling intensity as early as 30 min after exposure to MSA. The decrease was stable for at least 24 h. Cluster 3 consists of 19 proteins or 10% of the total; this cluster showed a gradual loss of reactive thiols starting at 30 min after MSA treatment and reached a nadir at 3 h. Interestingly, it rebounded rather quickly, and the label intensity returned towards the control value at 6 h. Cluster 4 consists of 15 proteins or 8% of the total; in this cluster there was a gain of reactive thiols at 3 h, followed by a rapid recovery to normal at 6 h. It is also important to note that the cells were not synchronized. Therefore the above redox changes could not be attributed to time-dependent progression of the cell cycle. For the sake of comparison, similar SOM clustering analysis with the control dataset did not reveal any distinguishing changes (Figure 7).

*Protein identification by mass spectrometry.* The mass spectrometry data of a total of 85 proteins are available at our website (http://falcon.roswellpark.org/publication/Park/Se_Proteomics/). These proteins are organized by the four SOM clusters in Table I, which also gives information on the accession number, protein name, subcellular localization, and vicinal thiols. There are 45 proteins identified in cluster 1, 25 in cluster 2, 9 in cluster 3, and 6 in cluster 4. The cluster 1 proteins are insensitive to MSA. Interestingly, of the 27 vicinal thiol-containing proteins and 64 vicinal thiol-sequences listed in Table I, 13 (48%) and 29 (45%), respectively, are in this cluster. The observation suggests that not all vicinal thiols are necessarily inviting targets for redox changes by selenium. The proteins in clusters 2, 3 and 4 are present in various subcellular compartments, including nucleus, cytoplasm, mitochondria and membranes. Their ubiquity is consistent with the pervasive nature of a small selenium metabolite capable of striking many sensitive targets in a cell. Individually, there could be changes in the function of these proteins when their redox status is altered. On a global scale, this magnitude of protein redox modification is likely to affect cellular responses, as discussed in the next section.

*Induction of chaperones by MSA.* Protein thiol redox modification is likely to lead to changes in protein conformation. This form of protein-damaging stress is known to induce the expression of chaperones. These are molecules charged with the dual functions of stress sensors and rescuing misfolded proteins. We have examined a panel of chaperones by Western blot analysis in control cells and MSA-treated cells. Figure 8 shows the data of five chaperones which were significantly induced by MSA. Of these, GRP170, GRP78 and PDI are present in the endoplasmic reticulum, while HSP70 (inducible) and HOP-p60 are present in the cytosol. The above observation suggests that the protein thiol redox changes induced by MSA are probably substantial enough to produce a cellular stress response. We also have additional data (not shown) indicating that HSP70 (constitutive), HSP90 and HSP110 were not increased by MSA. It is of interest to note that the five inducible chaperones (GRP170, GRP78, PDI, inducible HSP70 and HOP-p60) are generally present at low levels in control cells. In contrast, the three non-inducible chaperones (constitutive HSP70, HSP90 and HSP110) are generally present at high levels regardless of cell stress conditions.

## Discussion

This is the first study to report the use of a display thiol-proteomics approach to evaluate global protein redox modification by selenium. In spite of the novelty, there is a caveat to our research finding. Our methodology is limited to the detection of high abundance proteins. With few exceptions, low abundance proteins, proteins with extreme pI, or proteins with poor solubility, are generally not well resolved. Thus, in reality, the present approach is likely to under-estimate the number of redox-sensitive proteins. Not all reactive thiol-containing proteins are targets of selenium. Of the total of 194 proteins on our display, 51% showed little response (cluster 1), 41% showed a loss of reactive thiols (clusters 2 and 3), and 8% showed a gain of reactive thiols (cluster 4). Depending on the influence of neighboring groups and redox potential, the reactivity of protein thiols with methylselenolate can vary diametrically, such that the thiols can either be oxidized or reduced. The loss of reactive thiols (equivalent to thiol oxidation), especially under oxidative condition, might be represented by the following reactions:

$$Cys-S^- \xrightarrow{[o]} Cys-S^{\bullet} \xrightarrow{[CH_3Se^-]} Cys-S-SeCH_3 \xrightarrow{[Cys-SH]} Cys-S-S-Cys + CH_3Se^-$$

Indeed, our preliminary data (unpublished) showed that MSA produced a sustained increase of reactive oxygen species, and hence might favor the above reaction. Conversely, the reduction of protein disulfide by the highly nucleophilic methylselenolate would result in the gain of

Table I. *Protein identification by mass spectrometry.*

| SSP No. | Accession | Protein name | Subcellular location | Vicinal thiol |
|---|---|---|---|---|
| | | Cluster 1 | | |
| 201 | BAB21814 | KIAA1723 protein | | |
| 202 | P33459 | POL polyprotein contains protease Retropepsin | | 869-CEIC |
| 404 | P78621 | Cytokinesis protein sepA FH1 2 protein | | |
| 1201 | P14742 | Glucosamine fructose 6 phosphate aminotransferase | | 183-CKSC |
| 1304 | P40939 | Mitochondrial Trifunctional Enzyme alpha subunit precursor | Mitochondrial matrix | |
| 1601 | P43329 | ATP dependent helicase hrpA | | 1112-CISC |
| 1801 | NP_004125 | Heat shock 70kDa | | |
| 2103 | P32485 | Mitogen activated protein kinase HOG1 | | |
| 2304 | 4505773 | Prohibitin | | |
| 2404 | AAQ10304 | IL1RAPL1-dystrophin fusion protein | | |
| 2501 | Q10250 | Hypothetical 170 7 kDa protein C56F8 02 in chromosome I | Integral membrane protein (Potential) | 770-CVEC |
| 2807 | P38646 | Stress-70 protein, mitochondrial precursor | Mitochondrial | |
| 2809 | Q60577 | Heterogeneous nuclear ribonucleoprotein K | Cytoplasmic and nuclear; nucleoplasm | |
| 3205 | P32119 | Peroxiredoxin 2 | Cytoplasmic | |
| 3302 | P31937 | 3 hydroxyisobutyrate dehydrogenase mitochondrial precursor | Mitochondrial | |
| 3303 | O65607 | DNA mismatch repair protein MSH3 AtMsh3 | | |
| 3304 | P05164 | Myeloperoxidase precursor(MPO) C-1-tetrahydrofolate synthase, cytoplasmic | Lysosomal | 316-CPAC |
| 3305 | Q16658 | Fascin(actin bundling protein) | | |
| 3402 | Q9UY36 | Alanyl tRNA synthetase | | 20-CKVC |
| 3404 | P15531 | Nucleoside diphosphate kinase A | Nuclear and cytoplasmic | |
| 3701 | NP_005304 | Glucose regulated protein, 58kDa | | 57-CGHC, 406-CGHC |
| 3702 | P30101 | Protein disulfide isomerase A3 precusor | Endoplasmic reticulum lumen (By similarity) | 57-CGHC, 406-CGHC |
| 3801 | P38646 | Mitochondrial stress-70 protein precusor | Mitochondrial | |
| 3805 | O65607 | DNA mismatch repair protein MSH3 AtMsh3 | | |
| 4206 | P28649 | Cytochrome P450 11B1 mitochondrial precursor | Membrane-bound | |
| 4208 | P30048 | Thioredoxin dependent peroxide reductase mitochondrial | Mitochondrial | |
| 4301 | P30084 | Enoyl-CoA hydratase, Mitochondrial precursor | Mitochondrial matrix | |
| 4304 | P06713 | Nitrogen regulation protein | | |
| 4401 | BAB84979 | FLJ0226 protein | | |
| 4501 | P17545 | DNA directed RNA polymerase II largest subunit | Nuclear | 69-CETC, 107-CVCKTC |
| 4504 | P48681 | Nestin | | |
| 4608 | P78371 | T-complex protein 1, beta subunit | Cytoplasmic | |
| 4802 | P13433 | DNA directed RNA polymerase mitochondrial precursor | Mitochondrial | |
| 4805 | O19048 | DNA directed RNA polymerase II largest subunit | Nuclear (By similarity) | |
| 5301 | NP_005338 | Heat shock 70kDa protein 5 | | |
| 5806 | Q15942 | Zyxin | Cytoplasmic; associates with the actin cytoskeleton near the adhesion plaques | 384-CGRC, 409-CFTCHQC, 433-CEGC, 444-CNTC, 467-CFTCVVC, 504-CSVC, 534-CYKCEDC, 562-CRKC |
| 6301 | Q13490 | Inhibitor of apoptosis protein 2(HIAP2) | Cytoplasmic (Potential) | 83-CFCC, 220-CFAC, 306-CFCC, 571-CKVC, 592-CQEC, 602-CPIC |
| 6304 | Q9UPN3 | Microtubule-actin crosslinking factor 1, isoforms 1/2/3 | Cytoplasmic | 775-CLC, 5175-CKC |
| 6401 | P03519 | Matrix protein | | |
| 6402 | BAA22860 | A+U-rich element RNA binding factor | | |
| 6604 | P50995 | Annexin A11 Annexin XI Calcyclin associated annexin | Cytoplasmic and possibly nuclear | |
| 6701 | P78527 | DNA-dependent protein kinase catalytic subunit | Nuclear | 1029-CGRC |
| 6801 | P00558 | Phosphoglycerate kinase 1 | | |
| 6810 | NP_228019 | ABC transporter, ATP-binding protein | | |
| 7201 | NP_002565 | Peroxiredoxin 1 | | |
| 7301 | P25388 | Guanine nucleotide-binding protein beta subunit-like protein 12.3 | | |

| SSP No | Accession | Protein name | Subcellular location | Vicinal thiol |
|---|---|---|---|---|
| | | Cluster 2 | | |
| 105 | P39975 | Hypothetical 26 8 kDa protein in DLD3 5 region | | 4-CPC |
| 302 | AAL84570 | TPMsk3 | | |
| 1102 | Q15181 | Inorganic pyrophosphatase | Cytoplasmic (By similarity) | |
| 1103 | Q04832 | DNA binding protein HEXBP Hexamer binding protein | Nuclear | 18-CRNC, 45-CFRC, 72-CFRC, 99-CYKC, 142-CYKC, 170-CYKC, 198-CYKC, 224-CYKC, 255-CYKC |
| 1704 | P25328 | Probable RNA directed RNA polymerase in W dsRNA E | | 218-CEPC, 456-CRVC |
| 2102 | P47768 | DNA directed RNA polymerase beta chain | | |
| 2701 | P05209 | Tubulin alpha 1 chain | | |
| 3204 | P41958 | Apoptosis regulator ced 9 | | |
| 3306 | Q10451 | Hypothetical 141 9 kDa protein C12B10 18 in chromosome I | | 757-CYC |
| 3307 | Q45388 | TEX protein | | |
| 3604 | Q10970 | Chromosome partition protein smc | | |
| 4103 | P05092 | Peptidyl prolyl cis trans isomerase A | Cytoplasmic | |
| 4201 | NP_000260 | Nucleoside-diphosphate kinase 1 isoform b | | |
| 5101 | P20228 | Glutamate decarboxylase | | |
| 5202 | P52111 | Glycerol 3 phosphate dehydrogenase | Cytoplasmic | |
| 5303 | O31047 | Adenylosuccinate synthetase | Cytoplasmic (By similarity) | |
| 5601 | O33369 | DNA gyrase subunit B | Intergral membrane protein (Potential) | |
| 5805 | NP_005496 | Scavenger receptor class B, member 1; CD36 antigen-like 1 | | 321-CPC |
| 7101 | P04080 | Cystatin B Liver thiol proteinase inhibitor | Cytoplasmic and nuclear | |
| 7404 | Q9TT14 | Voltage dependent anion selective channel protein | Outer mitochondrial membrane (By similarity) | |
| 7704 | Q03265 | ATP synthase alpha chain mitochondrial precursor | Mitochondrial inner membrane | |
| 8104 | O18017 | Probable Bloom s syndrome protein homolog | Nuclear (By similarity) | 640-CDIC |
| 8201 | P37802 | Transgelin 2 SM22 alpha homolog | | |
| 8501 | P07954 | Fumarate hydratase | Mitochondrial and cytoplasmic | |
| | | Cluster 3 | | |
| 106 | Q20799 | Probable calcium binding mitochondrial carrier F55 | Integral membrane protein. (By similarity) | Mitochondrial inner membrane 448-CGTC |
| 107 | P08968 | DNA directed RNA polymerase III largest subunit E | Nuclear | 74-CETC, 114-CKRC, 161-CLKC, 495-CCC |
| 2401 | NP_000909 | Proline 4 hydroxylase | | 53-CGHC, 397-CGHC |
| 5401 | P06733 | Alpha enolase | Cytoplasmic | 337-CNC, |
| 7302 | Q99714 | 3 hydroxyacyl CoA dehydrogenase type II | | |
| 7303 | 229674 | Aldolase A | | |
| 7402 | P04406 | Glyceraldehyde 3-phosphate dehydrogenase, liver | Cytoplasmic | |
| 7504 | Q91187 | V D J recombination activating protein 1 | Nuclear | 110-CLCRLC, 176-CQRC, 207-CLLC, 310-CQVC, 330-CRSC, 345-CPAC, 762-CTLC |
| 7702 | O60701 | UDP glucose 6 dehydrogenase | | |
| | | Cluster 4 | | |
| 602 | Q05022 | rRNA biogenesis protein RRP5 | Nuclear; nucleolar | |
| 2305 | PMHUYM | Phosphoglycerate mutase | | |
| 3207 | P16666 | Inclusion body matrix protein Viroplasmin | Cytoplasmic inclusion bodies | 477-CHHC |
| 3405 | NP_003748 | Eukaryotic translation initiation factor 3, subunit 2 beta; TNF beta receptor interacting protein 1 | | |
| 5702 | NP_000427 | 3-oxoacidCoA transferase | | 28-CVC |
| 7801 | P78332 | RNA binding protein 6 RNA binding motif protein 6 | Nuclear (Probable) | 542-CKRC, 556-CSFC, 957-CLLC |

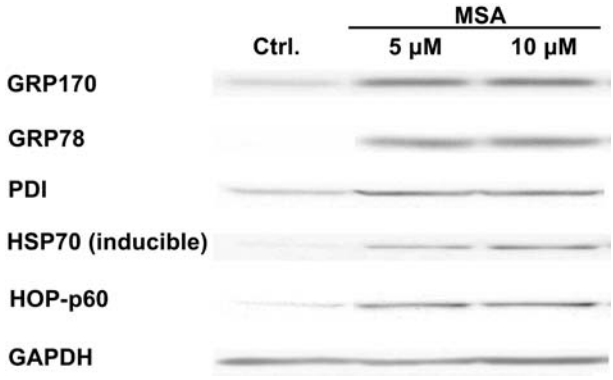


Figure 8. *Western blot analysis of chaperone expression in control or MSA-treated cells.*

reactive thiols: $Cys-S-S-Cys \xrightarrow{[CH_3Se^-]} Cys-S^- + CH_3Se-SX$

As depicted in Figure 6, a proportion of the redox-sensitive proteins reverted back to their basal thiol status within a short period of time. The recovery is probably due to repair by thiol-disulfide oxidoreductases. Thus, some of the damage does not appear to be too long lasting.

Redox regulation of proteins has a profound effect on their functions/activities. Two examples are cited below to illustrate how selenium causes defined redox changes which are accompanied by either a gain or loss of function/activity of the protein. Full length human p53 contains 10 cysteine residues. Using a 20 KDa carboxyl-terminal fragment of p53 with two cysteines at codons 275 and 277, Seo *et al.* (20) reported that a reduction of these two thiols by selenium significantly increases sequence specific DNA binding and transactivation of p53. MSA and selenite are more potent than selenomethionine in inducing p53 redox changes (21). The finding is congruent with the interpretation that MSA and selenite are converted to the reactive monomethylated metabolite much more efficiently than selenomethionine. A second example is provided by the work of Gopalakrishna *et al.* (22) regarding the redox modification of protein kinase C by selenite. There are two cysteine-rich regions in protein kinase C: the regulatory domain contains 12 cysteine residues, and the catalytic domain contains 6 or 7 cysteine residues. At low concentrations, selenite converts 4 cysteine residues to 2 disulfides; and at high concentrations, it converts 8 cysteine residues to 4 disulfides. The former modification is associated with a loss of affinity to ATP, while the latter with a lower $V_{max}$ of the enzyme.

Without doing similarly sophisticated biochemistry with the proteins of Table I, there is no way to predict how their functions or activities will be affected by thiol redox changes. Part of our future effort will be focused on this area of research. Depending on the redox milieu of the tissue, as well as that of the cellular and subcellular environment, selenium might act as a chemical switch to turn a protein on or off without affecting the expression level of the protein. On a grander scale, there is increasing recognition that many cellular processes are sensitive to the integration of redox signals. Global redox modification of protein thiols can be a major driving force of cellular stress, since these changes are likely to lead to protein unfolding, misfolding or aggregation. Protein-damaging stress is known to induce the expression of chaperones whose function is to rescue the misfolded proteins (23). The fact that we were able to detect increases in endoplasmic reticulum and cytosol chaperones in MSA-treated cells could mean that the rescue operation requires the assistance of extra chaperones. The endoplasmic reticulum (ER) is a particularly vulnerable site because this is the organelle for protein folding. An accumulation of misfolded or unfolded proteins in the ER can trigger an adaptive stress response which is associated with the induction of a defined set of sensors and modulators to stop protein synthesis and to refold or degrade the aberrant proteins (24-26). If the perturbation is too severe and beyond repair, effector signals are subsequently recruited to achieve cell cycle exit and apoptosis. Given what we know about cellular responses to selenium, we are currently pursuing the idea that stress signaling as a result of protein redox modification might be an early event which ultimately determines how cells respond to treatment with selenium.

## Acknowledgements

This work was supported by The Ralph C. Wilson, Sr. and Ralph C. Wilson, Jr. Medical Research Foundation, Korea Ministry of Science and Technology and grants CA 09796 and CA109480 from the National Cancer Institute, U.S.A.

## References

1 Combs GF and Clark LC: Selenium and cancer prevention. *In*: Antioxidant Nutrients and Disease Prevention Boca Raton, FL, CRC Press, 1997.

2 Ip C and Ganther HE: Activity of methylated forms of selenium in cancer prevention. Cancer Res *50*: 1206-1211, 1990.

3 Ip C, Hayes C, Budnick RM, and Ganther HE: Chemical form of selenium, critical metabolites, and cancer prevention. Cancer Res *51*: 595-600, 1991.

4 Ip C: Lessons from basic research in selenium and cancer prevention. J Nutr *128*: 1845-1854, 1998.

5 Ip C, Thompson HJ, Zhu Z and Ganther HE: *In vitro* and *in vivo* studies of methylseleninic acid: Evidence that a monomethylated selenium metabolite is critical for cancer chemoprevention. Cancer Res *60*: 2882-2886, 2000.

6 Dong Y, Zhang H, Hawthorn L, Ganther HE and Ip C: Delineation of the molecular basis for selenium-induced growth arrest in human prostate cancer cells by oligonucleotide array. Cancer Res *63*: 52-59, 2003.

7 Zu K and Ip C: Synergy between selenium and vitamin E in apoptosis induction is associated with activation of distinctive initiator caspases in human prostate cancer cells. Cancer Res *63*: 6988-6995, 2003.
8 Dong Y, Lee SO, Zhang H, Marshall J, Gao AC and Ip C: Prostate specific antigen (PSA) expression is down-regulated by selenium through disruption of androgen receptor signaling. Cancer Res *64*: 19-22, 2004.
9 Jiang C, Wang Z, Ganther H and Lu J: Caspases as key executors of methyl selenium-induced apoptosis (anoikis) of DU-145 prostate cancer cells. Cancer Res *61*: 3062-3070, 2001.
10 Jiang C, Wang Z, Ganther H and Lu J: Distinct effects of methylseleninic acid *versus* selenite on apoptosis, cell cycle, and protein kinase pathways in DU145 human prostate cancer cells. Mol Cancer Therapeut *1*: 1059-1066, 2002.
11 Wang Z, Jiang C and Lu J: Induction of caspase-mediated apoptosis and cell-cycle G1 arrest by selenium metabolite methylselenol. Mol Carcinogen *34*: 113-120, 2002.
12 Polgar L and Halasz P: Evidence for multiple reactive forms of papain. Eur J Biochem *88*: 513-521, 1978.
13 Page MG and West IC: Characterization *in vivo* of the reactive thiol groups of the lactose permease from *Escherichia coli* and a mutant; exposure, reactivity and the effects of substrate binding. Biochim Biophys Acta *858*: 67-82, 1986.
14 Wefers H and Sies H: Oxidation of glutathione by the superoxide radical to the disulfide and the sulfonate yielding singlet oxygen. Eur J Biochem *137*: 29-36, 1983.
15 Medeiros MH, Wefers H and Sies H: Generation of excited species catalyzed by horseradish peroxidase or hemin in the presence of reduced glutathione and $H_2O_2$. Free Radic Biol Med *3*: 107-110, 1987.
16 Ganther HE: Selenium metabolism, selenoproteins and mechanisms of cancer prevention: complexities with thioredoxin reductase. Carcinogenesis *20*: 1657-1666, 1999.
17 Kim JR, Yoon HW, Kwon KS, Lee SR and Rhee SG: Identification of proteins containing cysteine residues that are sensitive to oxidation by hydrogen peroxide at neutral pH. Anal Biochem *283*: 214-221, 2000.
18 Tamayo P, Slonim D, Mesirov J, Zhu Q, Dmitrovsky E, Lander ES and Golub TR: Intepreting gene expression with self-organizing maps: methods and application to hematopoeitic differentiation. Proc Natl Acad Sci USA *96*: 2907-2912, 1999.
19 Golub TR, Slonim DK, Tamayo P, Huard C, Gaasenbeek M, Mesirov JP, Coller H, Loh ML, Downing JR, Caligiuri MA, Bloomfield CD and Lander ES: Molecular classification of cancer: class discovery and class prediction by gene expression monitoring. Science *286*: 531-537, 1999.
20 Seo YR, Kelley MR and Smith ML: Selenomethionine regulation of p53 by a Ref1-dependent redox mechanism. Proc Natl Acad Sci USA *99*: 14548-14553, 2002.
21 Smith ML, Lancia JK, Mercer TI, Kelley MR and Ip C: Selenium compounds regulate p53 by common and distinctive mechanisms. Anticancer Res *24*: 1401-1408, 2004.
22 Gopalakrishna R, Gunimeda U and Chen Z-H: Cancer-preventive selenocompounds induce a specific redox modification of cysteine-rich regions in $Ca^{2+}$-dependent isoenzymes of protein kinase C. Arch Biochem Biophys *348*: 25-36, 1997.
23 Mosser DD and Morimoto RI: Molecular chaperones and the stress of oncogenesis. Oncogene *23*: 2907-2918, 2004.
24 Kaufman RJ: Orchestrating the unfolded protein response in health and disease. J Clin Invest *110*: 1389-1398, 2002.
25 Rao RV, Ellerby HM and Bredesen DE: Coupling endoplasmic reticulum stress to the cell death program. Cell Death Differ *11*: 372-380, 2004.
26 Shen X, Zhang K and Kaufman RJ: The unfolded protein response - a stress signaling pathway of the endoplasmic reticulum. J Chem Neuroanat *28*: 79-92, 2004.

*Received December 8, 2004*
*Accepted December 28, 2004*